crystals

MDPI

Article

Effect of Sintering Temperature on Microstructure and Mechanical Properties of Hot-Pressed Fe/$FeAl_2O_4$ Composite

Kuai Zhang [1,2], Yungang Li [1], Hongyan Yan [1,*], Chuang Wang [1], Hui Li [1], Jinglong Liang [1] and Jie Dang [3]

[1] College of Metallurgy and Energy, North China University of Science and Technology, Tangshan 063210, China; whh@qy.ncst.edu.cn (K.Z.); lyg@ncst.edu.cn (Y.L.); xiaoniji@163.com (C.W.); lh@ncst.edu.cn (H.L.); ljl@ncst.edu.cn (J.L.)
[2] College of Qinggong, North China University of Science and Technology, Tangshan 064000, China
[3] College of Materials Science and Engineering, Chongqing University, Chongqing 400044, China; jiedang@cqu.edu.cn
* Correspondence: yanhy@ncst.edu.cn

Abstract: An Fe/$FeAl_2O_4$ composite was prepared with Fe-Fe_2O_3-Al_2O_3 powder by a hot press sintering method. The mass ratio was 6:1:2, sintering pressure was 30 MPa, and holding time was 120 min. The raw materials for the powder particles were respectively 1 μm (Fe), 0.5 μm (Fe_2O_3), and 1 μm (Al_2O_3) in diameter. The effect of sintering temperature on the microstructure and mechanical properties of Fe/$FeAl_2O_4$ composite was studied. The results showed that Fe/$FeAl_2O_4$ composite was formed by in situ reaction at 1300 °C–1500 °C. With the increased sintering temperature, the microstructure and mechanical properties of the Fe/$FeAl_2O_4$ composite showed a change law that initially became better and then became worse. The best microstructure and optimal mechanical properties were obtained at 1400 °C. At this temperature, the grain size of Fe and $FeAl_2O_4$ phases in Fe/$FeAl_2O_4$ composite was uniform, the relative density was 96.7%, and the Vickers hardness and bending strength were 1.88 GPa and 280.0 MPa, respectively. The wettability between Fe and $FeAl_2O_4$ was enhanced with increased sintering temperature. And then the densification process was accelerated. Finally, the microstructure and mechanical properties of the Fe/$FeAl_2O_4$ composite were improved.

Keywords: sintering temperature; Fe/$FeAl_2O_4$ composite; hot press sintering; microstructure; mechanical properties

Citation: Zhang, K.; Li, Y.; Yan, H.; Wang, C.; Li, H.; Liang, J.; Dang, J. Effect of Sintering Temperature on Microstructure and Mechanical Properties of Hot-Pressed Fe/$FeAl_2O_4$ Composite. *Crystals* **2021**, *11*, 422. https://doi.org/10.3390/cryst11040422

Academic Editor: Indrajit Charit

Received: 25 March 2021
Accepted: 11 April 2021
Published: 14 April 2021

1. Introduction

An iron-based composite takes iron as the continuous matrix, ceramic particles as the dispersed reinforcement, and the reinforcement particles are uniformly distributed in the matrix [1–3]. Based on the high hardness and strength of ceramic particles, such as Al_2O_3 and $FeAl_2O_4$, the hardness of the material will improve on the basis of excellent toughness after wetting between iron and ceramic phases, which shows some common properties of metals and ceramics, and can find a wide range of application, including braking, sealing, cutting, loading and other fields [4–8].

In 1959, Gatti [9] prepared the world's first Fe-based composite using Fe and Al_2O_3 powers as raw material. However, it was difficult to combine the metal and ceramic phases with wetting, due to the different material properties of metal and ceramic, such as the difference in thermal expansion coefficient [10].

In order to solve the problem of wetting, it has been found that the wettability between $FeAl_2O_4$ (Fe-Al spinel) and Fe phase is better after the formation of $FeAl_2O_4$ (Fe-Al spinel) [11]. Spinel clusters are generally formed on the ceramic-metal interface and grow inside and outside in the form of particles. The more $FeAl_2O_4$, the better the fracture toughness of the cermet [12–14]. However, in the Fe-O-Al system, there are five phases of fusterite, iron spinel, Fe_2O_3, Al_2O_3, and $Fe_2O_3 \cdot Al_2O_3$. The spinel phase exists as a series of

continuous solid solutions between $FeAl_2O_4$ and Fe_3O_4 [15]. The prerequisite for the stable existence of $FeAl_2O_4$ is that FeO can exist stably. The sintering temperature also plays an important role [16]. Trumble [17] conducted a thermodynamic analysis on the reaction of $FeAl_2O_4$ at the interface and pointed out that $FeAl_2O_4$ would form and exist stably below 1600 °C. Chen [18] focused on the specific study of the formation and the thermodynamic conditions of FeO and $FeAl_2O_4$. It has been found that FeO existed stably in a suitable weak reducing atmosphere at 1427 °C, and spontaneously generated $FeAl_2O_4$ with Al_2O_3. Zhang [19] successfully prepared $FeAl_2O_4$ in a suitable weak reducing atmosphere. Using iron scales and bauxite as raw materials, Liu [20] also successfully prepared $FeAl_2O_4$ by sintering at 1550 °C. In fact, in the Fe, Fe_2O_3, and Al_2O_3 systems, the sintering temperature not only affects the formation of the spinel phase but also plays an important role in improving the wettability between the iron and ceramic phases.

In this study, vacuum hot pressing and sintering were used to add a reinforcing Fe_2O_3 phase to the Fe/Al_2O_3 system, and $FeAl_2O_4$ was formed by the in situ reaction of Fe, Fe_2O_3, and Al_2O_3 to improve the wettability between Fe and the ceramic phase. With the increased sintering temperature, the metal Fe changed from solid to liquid. The microstructure and mechanical properties of the $Fe/FeAl_2O_4$ composite were affected by the promotion of element diffusion, migration, and crystallization process. In order to obtain excellent properties of the $Fe/FeAl_2O_4$ composite, it was necessary to study the influence of sintering temperature on the microstructure and mechanical properties during the preparation of the $Fe/FeAl_2O_4$ composite.

2. Materials and Methods

The raw materials in this experiment were analytically pure Fe powder (1μm), Fe_2O_3 powder (0.5 μm), and Al_2O_3 powder (1 μm). The mass ratio of the Fe, Fe_2O_3, and Al_2O_3 powder was 6:1:2. Absolute ethanol was used as the dispersion medium, and a XQM-2 vertical planetary ball mill was used for ball milling. The ball milling speed was 300 r/min, and the ball milling time was 10 h. After ball milling, the samples were placed in a DZF-6050 vacuum drying oven at 120 °C for 24 h, and the vacuum was pumped to 100 Pa during drying. After drying, the mixed powder was passed through a 200-mesh sieve and put into a ZT-40-21Y high-temperature hot press sintering furnace to prepare the $Fe/FeAl_2O_4$ at 1300 °C, 1350 °C, 1400 °C, 1450 °C, 1500 °C, 30 MPa for 120 min, and the vacuum was pumped to 10^{-2} Pa during sintering. The experimental conditions of the five samples are shown in Table 1.

Table 1. Experimental conditions for each sample.

Sample	*T*/°C	*t*/min	Pressure/MPa	Mass Ratio
S1	1300	120	30	6:1:2
S2	1350	120	30	6:1:2
S3	1400	120	30	6:1:2
S4	1450	120	30	6:1:2
S5	1500	120	30	6:1:2

The relative density of the prepared samples was measured by the Archimedes principle, the bending strength was measured using the three-point bending method with a CMT4202 universal material testing machine with a crosshead speed of 0.5 mm/min and span of 30 mm, and the Vickers hardness was measured at a loading force of 49.05 N (5 kg) for 10–15 s by the Tukon2500 Vickers hardness tester. Phase and composition analyses (XPert PRO MPD, PANalytical, Netherlands) were carried out with an x-Ray diffractometer. The microstructure and element analyses were carried out with SEM and EDS (GeminiSEM 300, Zeiss, Germany), respectively.

3. Results and Discussion

3.1. Preparation Principle of Fe/$FeAl_2O_4$ Composite

Using the analysis of thermodynamic software HSC6.0, it was shown that Fe, Fe_2O_3, and Al_2O_3 powder can spontaneously synthesize $FeAl_2O_4$ through an in situ reaction under the experimental conditions, as shown in the following reaction (1):

$$\frac{1}{3}Fe + \frac{1}{3}Fe_2O_3 + Al_2O_3 = FeAl_2O_4 \quad \Delta G^{\theta} = -56.09 - 0.00621T\left(kJ{\cdot}mol^{-1}\right) \tag{1}$$

Due to the excessive Fe content in the mixed powder of ingredients, Fe_2O_3 and Al_2O_3 reacted completely after the in situ reaction and the Fe became redundant. The $FeAl_2O_4$ produced by the in situ reaction combined with the redundant metal Fe and the Fe/$FeAl_2O_4$ composite was prepared during the process of hot pressing and sintering. The in situ reaction occurred on the three-phase interface of Fe liquid, Fe_2O_3, and Al_2O_3. This was an interface reaction-driven wetting, according to the free energy change control theory of interface reaction proposed by Aksay [21], the solid-liquid interface energy can be expressed as Equation (2) [22,23]:

$$\sigma_{SL} = \sigma_{SL}^{0} + \frac{\Delta G_r}{A} \tag{2}$$

where σ_{SL}^{0} is the solid/liquid interface energy before the reaction, A is the interface area, and ΔG_r is the free energy change produced by the interface reaction product per unit volume. According to Aksay [21], the decrease of free energy in the interfacial reaction is the main driving force controlling the wetting process. The improvement of wettability is caused by the decrease of free energy. The interfacial reaction is more intense, ΔG_r is lower, and the wettability of the system is better.

For Reaction (1), ΔG^{θ} lowers with increased reaction temperature. Then, when the in situ reaction of $FeAl_2O_4$ is more intense, it would reduce ΔG_r and enhance the wettability of Fe liquid and $FeAl_2O_4$. With the wetting of Fe and $FeAl_2O_4$, the diffusion rate of Fe to $FeAl_2O_4$ grains accelerated. The rule is that as the $FeAl_2O_4$ grains grow up, Fe accumulates in the $FeAl_2O_4$ grains, which has a greater impact on the combination of Fe and $FeAl_2O_4$ phase at the macro level, and this is reflected in changes in microstructure and mechanical properties.

Figure 1 shows the normalized XRD results of each sample (S1–S5) prepared by hot press sintering at different sintering temperatures. The results show that the phase composition of each sample was phase Fe and $FeAl_2O_4$. At different sintering temperatures, the relative intensity of the $FeAl_2O_4$ diffraction peak was relatively stable, which means that in the S1–S5 samples, $FeAl_2O_4$ could be formed smoothly. With the occurrence of in situ reaction and the formation of $FeAl_2O_4$, the diffusion barrier from Fe to $FeAl_2O_4$ was broken. As the sintering temperature increased, the wettability between Fe and $FeAl_2O_4$ was improved, which would promote the migration of Fe to $FeAl_2O_4$ and strengthen the bonding ability between the metal phase and the ceramic phase.

3.2. Effect on Microstructure

Figure 2 shows the fracture structure of different samples prepared at different temperatures, which could characterize the combination of the metal phase and ceramic phase to a certain extent. The fracture of the Fe/$FeAl_2O_4$ composite was mainly intergranular. With increased sintering temperature, the microstructure of samples changed significantly.

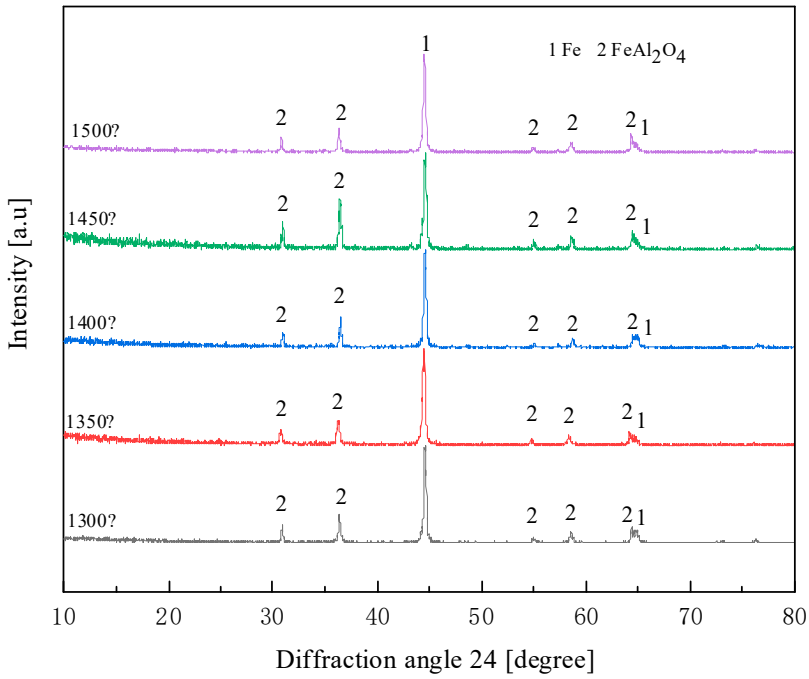

Figure 1. Normalized XRD patterns of $Fe/FeAl_2O_4$ composites with different temperatures.

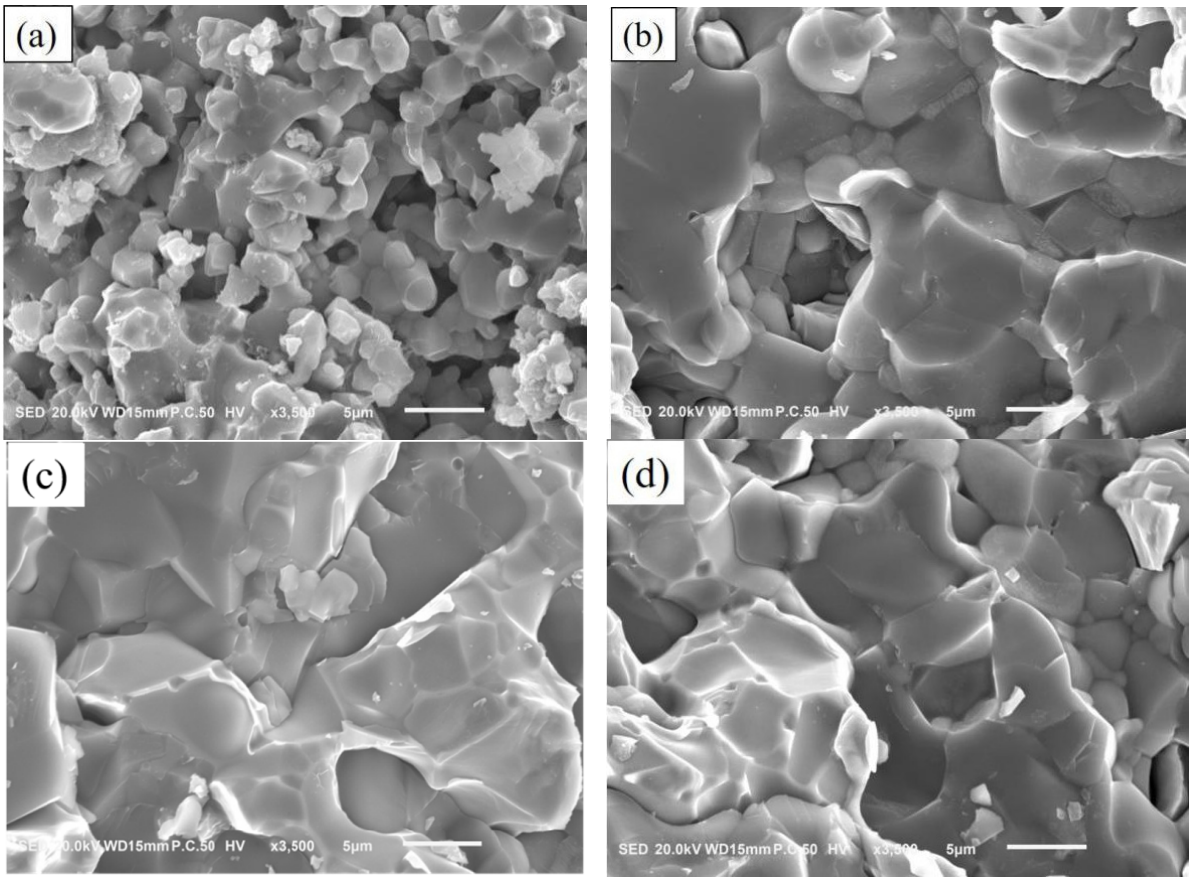

Figure 2. *Cont.*

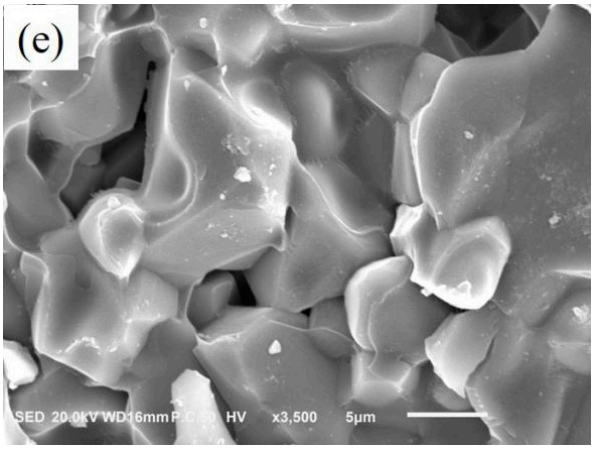

Figure 2. SEM micrographs of the fracture surface of Fe/$FeAl_2O_4$ composites with different temperatures: (**a**) 1300 °C, (**b**) 1350 °C, (**c**) 1400 °C, (**d**) 1450 °C, (**e**) 1500 °C.

At 1300 °C, a large number of grain boundaries exposed in the matrix and Fe phase could not bond $FeAl_2O_4$ grains effectively in the matrix. There were many pores in the sample and the density of the material was low. Increasing the sintering temperature from 1350 °C to 1450 °C, with the improvement of wettability, the number of pores decreased and the interface bonding between Fe and $FeAl_2O_4$ improved significantly. The grains of the two phases grew up obviously, and the Fe phase was continuously distributed at the grain boundary and three bifurcations of the $FeAl_2O_4$. Compared with the samples prepared at 1350 °C and 1450 °C, the sample sintered at 1400 °C showed the best micromorphology. When the sintering temperature reached 1500 °C, Fe grains began to become coarser, the surface of $FeAl_2O_4$ grains appeared powdered, and more pores appeared. The increase in sintering temperature affected the physical and chemical reactions in the hot press sintering process. On the one hand, it promoted the in situ reaction, reduced the interfacial energy of the solid/liquid surface, and improved the wettability of Fe and $FeAl_2O_4$. On the other hand, it enhanced the diffusion and migration ability of Fe, including the self-diffusion of the Fe phase and the diffusion of Fe to the $FeAl_2O_4$ phase, which promoted the nucleation and recrystallization processes of the Fe phase and $FeAl_2O_4$ phase.

The analysis results of the point scan and the surface scan of the energy spectrum in the sample prepared at 1400 °C are shown in Figures 3 and 4. The surface scanning (Figure 4) showed that the bright area was the Fe phase, and the dark area was the $FeAl_2O_4$ phase. The grains of Fe and $FeAl_2O_4$ were uniformly staggered, and the Fe phase presented strong continuity, which played a good bonding effect. At the same time, the Fe concentration area was obvious in the area with uniform distribution of $FeAl_2O_4$, indicating that the Fe diffused into the $FeAl_2O_4$ grains during the in situ reaction process. Combined with the EDS spot scanning results (Figure 3b), it could also be proved that the content ratio of Fe in the $FeAl_2O_4$ grains was excessive. At the sintering temperature of 1400 °C, the contact between Fe and $FeAl_2O_4$ phase could promote the diffusion and migration of the Fe to $FeAl_2O_4$, which enhanced the bonding ability between Fe and $FeAl_2O_4$. The wetting process followed the reaction-driven wetting mechanism, which improved the wettability between the two phases. This is consistent with the interface reaction free energy change control theory proposed by Aksay [21].

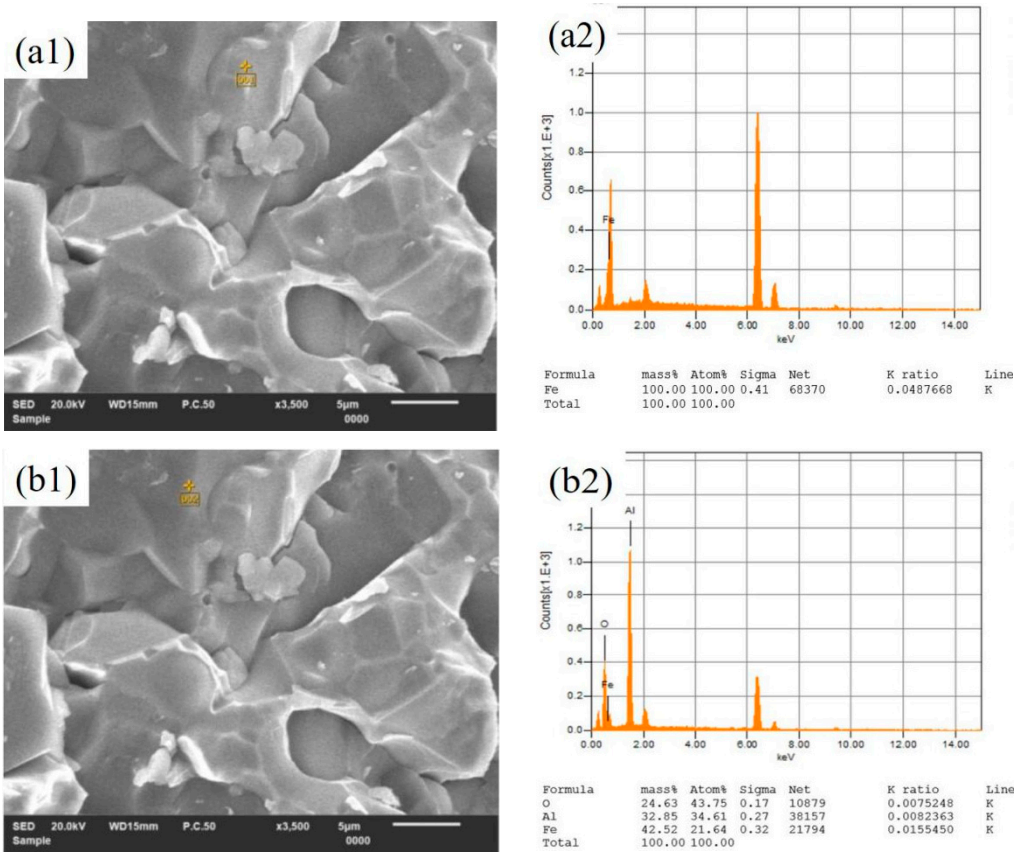

Figure 3. EDS analysis of $Fe/FeAl_2O_4$ composites at 1400 °C: (**a1**) Fe phase, (**a2**) EDS analysis of Fe phase, (**b1**) $FeAl_2O_4$ phase, (**b2**) EDS analysis of $FeAl_2O_4$ phase.

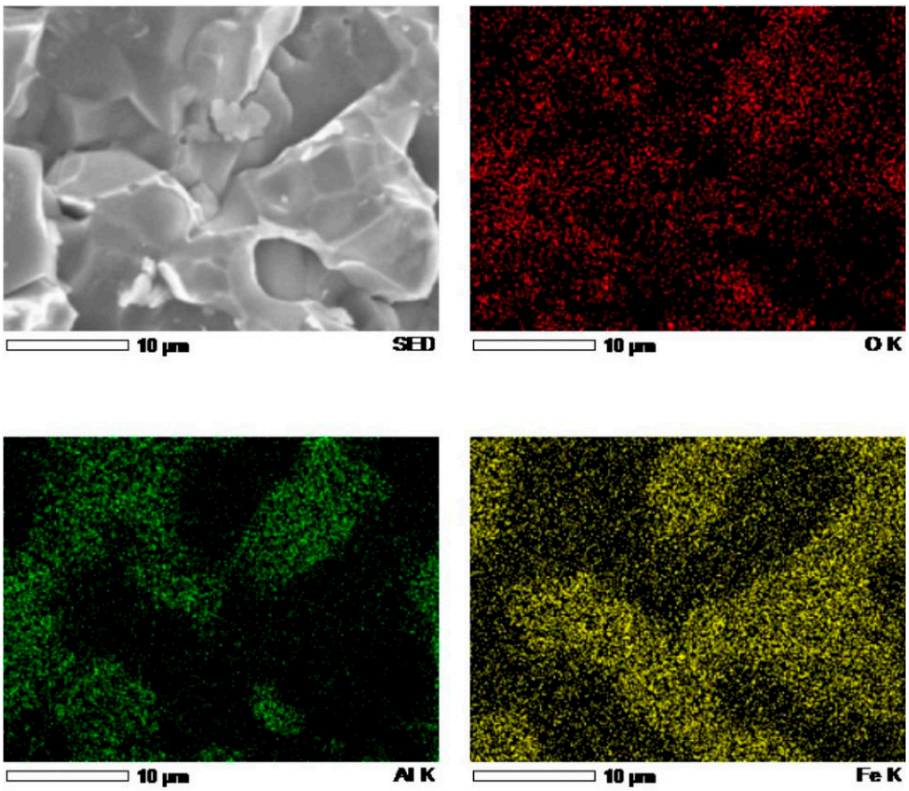

Figure 4. Mapping analysis for the major elements (Fe, Al, O) of $Fe/FeAl_2O_4$ composites at 1400 °C.

3.3. Effect on Mechanical Properties

The mechanical properties of the Fe/$FeAl_2O_4$ composites prepared at different sintering temperatures are shown in Figure 5. The results show that the relative density, Vickers hardness, and bending strength of the Fe/$FeAl_2O_4$ composite increased first and then decreased with the increasing sintering temperature. At 1400 °C, the relative density of the composite reached the maximum value of 96.7%. The microstructure of the composites is the main factor affecting the properties of the composites. The Vickers hardness and bending strength of the composites are also closely related to the density. With the increase in the relative density, the Vickers hardness and bending strength of the composites increased gradually and reached the maximum value of 1.88 GPa and 280.0 MPa at 1400 °C, respectively. However, when the sintering temperature increased to 1500 °C, the number of microscopic pores increased, which led to the decrease of the relative density, Vickers hardness, and bending strength of the Fe/$FeAl_2O_4$ composite.

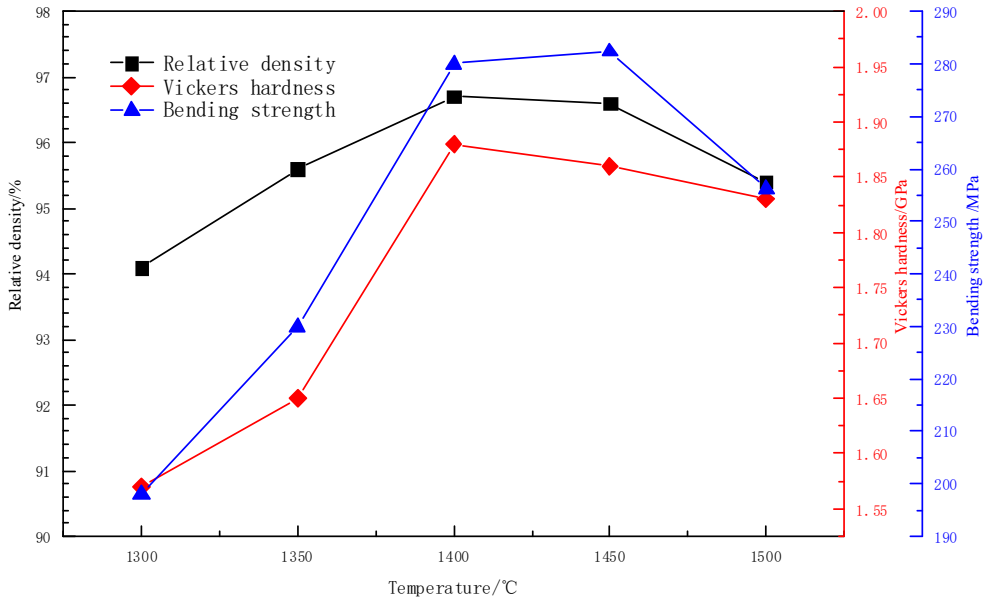

Figure 5. Effects of different temperatures on the relative density, Vickers hardness, and flexural strength of Fe/$FeAl_2O_4$ composites.

The effect of the sintering temperature on the mechanical properties of the Fe/$FeAl_2O_4$ composite can be explained using a dynamical theory for diffusion during mass transfer [24,25]:

$$\frac{\Delta V}{V} = 3\left(\frac{5\gamma\Omega D^*}{kT}\right)^{2/5} r^{-5/6} t^{2/5} \quad (3)$$

In Equation (3), $\frac{\Delta V}{V}$ is the shrinkage of the sample volume; Ω is the volume of vacancies; D^* is the self-diffusion coefficient; γ is the surface tension; k is the proportionality constant; T, r, and t are the temperature, the particle diameter, and the holding time, respectively. Equation (3) shows an exponential relationship between the sintering temperature and the relative density (set the holding as 120min), that is, increasing the sintering temperature can effectively improve the relative density of the Fe/$FeAl_2O_4$ composite. When the sintering temperature increased from 1300 °C to 1450 °C, the porosity of the cross section decreased obviously, and the relative density of the Fe/$FeAl_2O_4$ composite increased from 94.1% to 96.7%. In the temperature range of 1300 °C~1450 °C, the in situ reaction of $FeAl_2O_4$ was the rate-limiting link. The diffusion barrier of Fe to $FeAl_2O_4$ phase was broken by the in situ reaction and the wettability between Fe and $FeAl_2O_4$ was improved by increasing the sintering temperature, which accelerated the densification process and improved the mechanical properties of the composite. However, when the sintering temperature rose to 1500 °C, there were many obvious closed pores that remained

in the composite, and the relative density of $Fe/FeAl_2O_4$ composite decreased to 95.4%. According to the grain growth rate formula (4):

$$\nu = k\left(\frac{1}{r_1} + \frac{1}{r_2}\right)\exp\left(\frac{-\Delta G^*}{RT}\right) \quad (4)$$

where, k is a constant, r is the curvature radius of the surface, and ΔG^* is the atomic transition barrier. It can be seen from Formula (4) that with the increase of sintering temperature, the grain growth rate accelerates. When the sintering temperature was increased to 1500 °C, the diffusion of Fe became the rate-limiting link. The self-diffusion of Fe caused Fe grains to grow abnormally, and the speed of grain boundary movement increased, while the movement speed of pores was limited, which made it difficult to remove. Closed pores began to form in the composite, resulting in a decrease in the density of the composite material. At the same time, the accelerated diffusion of Fe to $FeAl_2O_4$ caused the structure of the $FeAl_2O_4$ grains to collapse, which deteriorated the mechanical properties of the composite. In this study, the optimum sintering temperature was 1400 °C.

4. Conclusions

In this paper, an $Fe/FeAl_2O_4$ composite was prepared by hot press sintering at different temperatures. The effect of sintering temperature on the phase formation, microstructure, and mechanical properties of the $Fe/FeAl_2O_4$ composite and the mechanism of action were studied. The following conclusions were obtained:

(1) When the sintering temperature increased from 1300 °C to 1450 °C, the wettability between Fe and $FeAl_2O_4$ was improved and the diffusion of Fe to $FeAl_2O_4$ was obviously promoted. As a result, the bonding ability of Fe and $FeAl_2O_4$ was enhanced. However, when the temperature increased to 1500 °C, Fe grains began to grow up abnormally, $FeAl_2O_4$ structure started to collapse and more pores remained in the $Fe/FeAl_2O_4$ composite. The bonding ability of Fe and $FeAl_2O_4$ began to decline.

(2) With the increase of sintering temperature, the relative density, Vickers hardness, and bending strength of $Fe/FeAl_2O_4$ composite first increased and then decreased. The best microstructure and mechanical properties were obtained at 1400 °C. At this temperature, the grain size of Fe and $FeAl_2O_4$ phases in composites was uniform, the relative density was 96.7%, and the Vickers hardness and bending strength were 1.88 GPa and 280.0 MPa, respectively.

(3) The mechanism of sintering temperature on the preparation of $Fe/FeAl_2O_4$ composite by hot press sintering was mainly to break the diffusion barrier of the Fe to $FeAl_2O_4$ phase by the in situ reaction and then improve the wettability between Fe and $FeAl_2O_4$. Appropriate sintering temperature could accelerate the densification process and improve the microstructure and mechanical properties of $Fe/FeAl_2O_4$ composites finally.

Author Contributions: K.Z. and C.W. conceived and designed the experiments; Y.L. and H.Y. analyzed the data; H.Y. wrote the paper; H.L. and J.L. guided the experiment; J.D. reviewed the paper. All authors have read and agreed to the published version of the manuscript.

Funding: This research was funded by the National Natural Science Foundation of China, grant number 51804126.

Institutional Review Board Statement: Not applicable.

Informed Consent Statement: Not applicable.

Data Availability Statement: Not applicable.

Acknowledgments: This work was supported by the National Natural Science Foundation of China (No. 51804126).

Conflicts of Interest: The authors declare they have no conflict of interest. The funders had no role in the design of the study; in the collection, analysis, or interpretation of data; in the writing of the manuscript; or in the decision to publish the results.

References

1. Shi, G.Q.; Ding, P.D.; Tang, J.X. The study of the microstructure and properties of iron-based metal and ceramic composite material. *J. Chongqing Univ. (Nat. Sci. Ed.)* **1995**, *18*, 55–60.
2. Rosso, M. Ceramic and metal matrix composites: Routes and properties. *J. Mater. Process. Technol.* **2006**, *175*, 364–375. [CrossRef]
3. Reshetenko, T.V.; Avdeeva, L.B.; Khassin, A.A.; Kustova, G.N.; Ushakov, V.A.; Moroz, E.M.; Shmakov, A.N.; Kriventsov, V.V.; Kochubey, D.I.; Pavlyukhin, Y.T. Coprecipitated iron-containing catalysts (Fe-Al_2O_3, Fe-Co-Al_2O_3, Fe-Ni-Al_2O_3) for methane decomposition at moderate temperatures I. Genesis of calcined and reduced catalysts. *Appl. Catal. A* **2004**, *268*, 127–138. [CrossRef]
4. Shi, Z.L.; Du, X.K.; Yu, H.R.; Li, C.A. Study on the microstructure and properties of iron-base metal-ceramic braking materials. *J. Lanzhou Univ. (Nat. Sci.)* **2001**, *37*, 36–41.
5. Shi, Z.L.; Zhang, G.Q.; Du, X.K.; Li, C.A. Study of the tribological behaviors of iron based metal ceramic composites. *J. Lanzhou Univ. (Nat. Sci.)* **2002**, *38*, 39–43.
6. Shi, Z.L.; Du, X.K.; Li, C.A. Fabrication and properties of the iron-based metal-ceramic braking materials for high-speed train. *J. Lanzhou Univ. (Nat. Sci.)* **2000**, *19*, 82–84.
7. Shi, Z.L.; Du, X.K.; Li, C.A. Study on the iron base ceramic metal braking materials for high-speed train. *J. China Railw. Soc.* **2001**, *23*, 29–32.
8. Wang, X.F.; Li, D.S. Iron-composite friction materials for aircraft application. *Mater. Eng.* **1999**, *3*, 27–29.
9. Gatti, A. Iron-alumina materials. *Trans. AIME* **1959**, *215*, 753–755.
10. Chen, W.P.; Yang, S.F.; Han, M.Y. Research development of ceramic/Fe-based alloy composites. *Chin. J. Nonferrous Met.* **2010**, *20*, 257–265.
11. Bansal, C. Metal-to-ceramic bonding in (Al_2O_3+Fe) composite studied by Miissbauer spectroscopy. *Bull. Mater. Sci.* **1984**, *6*, 13–16. [CrossRef]
12. Konopka, K.; Ozieblo, A. Microstructure and the fracture toughness of the Al_2O_3-Fe composites. *Mater. Charact.* **2001**, *46*, 125–129. [CrossRef]
13. Wang, Z.; Liu, J.F.; Ding, Y.S. Fabrication and Properties of Fe/Al_2O_3 Composites. *Chin. J. Mater. Res.* **2012**, *26*, 206–210.
14. Konopka, K. Shape, size and distribution of metal particles embedded in a ceramic matrix. *Solid State Phenom.* **2015**, *231*, 57–63. [CrossRef]
15. Atlas, L.M.; Sumida, W.K. Solidus, Subsolidus, and Subdissociation Phase Equilibria in the System Fe-Al-O. *Am. Ceram. Soc. Atlas Sumida.* **1958**, *41*, 150–160. [CrossRef]
16. Gupta, P.; Kumar, D.; Quraishi, M.A.; Parkash, O. Corrosion behavior of Al_2O_3 reinforced Fe metal matrix nanocomposites produced by powder metallurgy technique. *Adv. Sci. Eng. Med.* **2013**, *5*, 366–370. [CrossRef]
17. Trumblei, K.P. Thermodynamic Analysis of Aluminate Formation at Fe/Al_2O_3 and Cu/Al_2O_3 Interfaces. *Acta Met. mater.* **1992**, *40*, S105–S110. [CrossRef]
18. Chen, Z.Y.; Chai, J.L.; Li, Y. Formations of ferrous oxide and hercynite. *Naihuo Cailiao.* **2005**, *39*, 207–210.
19. Zhang, J.B.; Zhang, G.; Xiao, G.Q. Preparation of hercynite. *Bull. Chin. Ceram. Soc.* **2007**, *26*, 1003–1006.
20. Liu, H.L.; Li, Y.; Cao, H.F.; Ren, X.Y.; Shen, W.P. Sintering synthesis of hercynite clinker. *Naihuo Cailiao.* **2003**, *37*, 333–335.
21. Aksay, I.A.; Hoge, C.E.; Pask, J.A. Wetting under chemical-equilibrium and nonequilibrium conditions. *J. Phys. Chem.* **1976**, *78*, 1178–1183. [CrossRef]
22. Qu, W.; Fang, T.X. Advances in the wettability research of metal /ceramic systems: Experimental characterization and theoretical Estimation. *Mater. Rep.* **2019**, *33*, 3606–3612.
23. Liu, X.Y. Research on the wettability and interfacial interaction between Ti-Al molten alloys and ceramics. *Chongqing Univ.* **2016**, *3*, 11. [CrossRef]
24. Zhang, M.; Zhou, Z.H.; Yuan, T.C.; Li, R.D.; Zhang, W.S.; Zhang, Y.J.; Wang, M.B.; Xie, S.Y. Analysis of abnormal grain growth behavior during hot-press sintering of boron carbide. *Ceram. Int.* **2020**, *46*, 16345–16353. [CrossRef]
25. Zhang, X.; Han, X.Y.; Zhang, Y.D.; Liang, J.L.; Wang, C.; Liang, J.S. Effect of holding time and pressure on the densification, microstructure and mechanical properties of hot pressed Al_2O_3-CA_6-ZrO_2/Ni multi-phase composites. *J. Alloys Compd.* **2021**, *850*, 1–10. [CrossRef]